Mater. Res. Soc. Symp. Proc. Vol. 1325 © 2011 Materials Research Society
DOI: 10.1557/opl.2011.849

Thermoelectric Properties of Er-doped InGaN Alloys for High Temperature Applications

K. Aryal, I. W. Feng, B. N. Pantha, J. Li, J. Y. Lin, and H. X. Jiang

Department of Electrical and Computer Engineering, Texas Tech University, Lubbock, TX, 79409

ABSTRACT

Thermoelectric (TE) properties of erbium-silicon co-doped $In_xGa_{1-x}N$ alloys ($In_xGa_{1-x}N$: Er + Si, $0 \leq x \leq 0.14$), grown by metal organic chemical vapor deposition, have been investigated. It was found that doping of InGaN alloys with Er atoms of concentration, N[Er] larger than $5x10^{19}$ cm^{-3}, has substantially reduced the thermal conductivity, κ, in low In content InGaN alloys. It was observed that κ decreases as N[Er] increases in Si co-doped $In_{0.10}Ga_{0.90}N$ alloys. A room temperature ZT value of ~0.05 was obtained in $In_{0.14}Ga_{0.86}N$: Er + Si, which is much higher than that obtained in un-doped InGaN with similar In content. Since low In content InGaN is stable at high temperatures, these Er+Si co-doped InGaN alloys could be promising TE materials for high temperature applications.

INTRODUCTION

The recent developments of advanced thermoelectric (TE) materials and devices draws a lot of attention in power generation and solid-state cooling based on TE effects. They have potential applications in waste heat recovery, air conditioning, and refrigeration [1]. Thermopower generation has the advantages of no moving parts and environmental friendliness. However, applications of TE materials are still limited due to their relatively low efficiency [2]. The efficiency of a TE material is evaluated by the dimensionless figure of merit as follows;

$$ZT = \frac{\sigma S^2 T}{\kappa} \qquad (1)$$

where S, σ, κ, and T are the Seebeck coefficient, electrical conductivity, thermal conductivity, and absolute temperature, respectively [3-4]. In order to achieve high ZT, S should be large so that a small temperature difference can create a large voltage, σ should be large to minimize the Joule's heating, and κ should be small to decrease heat leakage and maintain a large temperature difference. Most of the ZT enhancements have been achieved by reducing κ. Nano-structure incorporation, supperlattice, nanowires, and the substitution of heavier elements are some of the methods used to reduce κ [5-14]

Currently Bi_2Te_3 based materials are widely used in TE technology due to their superior properties [15-17]. However, their operational temperature is limited to near room temperature. They are not suitable for power generation, which involves environments of high temperature operation. SiGe alloys are currently the prime choice for high temperature applications of power generation via TE technology but they have low efficiency [18-19].

Recently, III-nitride materials have attracted attention as potential TE materials for high temperature applications due to stablity at high temperatures, chemical inertness, mechanical hardness, and nontoxicity [20]. Furthermore, III-nitride based thin film TE devices could directly integrate with nitride high power devices for spot cooling where their performance is deteriorated by severe heating [21]. We have previously demonstrated that $In_xGa_{1-x}N$ with In content (In = 0.36) has a ZT value as good as SiGe alloys in a measured temperature range (300 to 450 K). However, such a high In content with a growth temperature of ~ 950 K may not be stable for prolonged high temperature operation above 1000 K [22-23]. In order to use InGaN as a TE material for high temperature applications, In content in InGaN alloys needs to be lowered. Since low In content has a high κ, this results in a low ZT. Doping of rare-earth elements has been investigated in other TE materials to enhance Seebeck coefficients and reduce κ [24]. ErAs as nanoparticles embedded in $In_{0.53}Ga_{0.47}As$ alloys have been found to have a reduced κ compared with that of alloys without those particles [25]. Here, we investigate TE properties of $In_xGa_{1-x}N$:Er+Si alloys for potential in high temperature applications.

EXPERIMENTAL DETAILS

$In_xGa_{1-x}N$: Er+Si alloys were grown on semi-insulating c-GaN/sapphire templates by metal organic chemical vapor deposition (MOCVD). $In_xGa_{1-x}N$ alloys of thickness ~ 0.2 μm were doped by Er with a concentration > $5x10^{19}cm^{-3}$. Since Er doped InGaN alloys are highly resistive, we co-doped these alloys with Si. Trimethylgallium (TMGa) and Trimethylindium (TMIn) were used as precursors for Ga and In, respectively. Nitrogen and hydrogen were used as carrier gases for InGaN and GaN, respectively. For an active nitrogen source, high purity ammonia was used.

Seebeck coefficient S and thermal conductivity κ of $In_xGa_{1-x}N$: Er+Si were measured by thermal gradient and 3ω methods [26-27] which have been described previously [22-23]. A 150 nm SiO_2 layer was deposited on the surface of both $In_xGa_{1-x}N$: Er+Si samples and GaN/sapphire templates (reference samples) by plasma enhanced chemical vapor deposition (PECVD), which provides insulation for 3ω measurements. Identical heater/sensor patterns on both the actual and reference samples were made by developing a heater pattern with optical lithography and depositing 20 nm Ni/120 nm Au and lift-off techniques. The width and length of heaters were 20 μm and 1000 μm, respectively. In order to apply sinusoidal current with frequency ω, a digital lock-in amplifier was used and the voltages corresponding to ω and 3ω components were collected across the metal heater. An optical image of the heater/sensor pattern, the layer structure, and in-phase components of ac temperature oscillation for an actual and a reference sample are shown in Fig. 1.

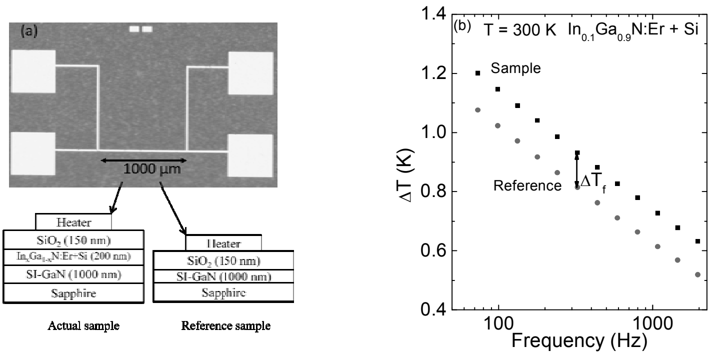

Fig. 1 (a) Optical image of a fabricated heater for 3ω measurement and layer structures of an actual and a reference samples; (b) In-phase components of the temperature oscillation (ΔT) as a function of frequency of ac current at room temperature for the reference (GaN/sapphire template) and the actual sample ($In_{0.10}Ga_{0.90}N$: Er +Si grown on GaN/sapphire template).

RESULTS AND DISCUSSION

Figure 2 shows the measured κ of $In_xGa_{1-x}N$:Er+Si as a function of x for x up to 0.35. κ of un-doped $In_xGa_{1-x}N$ alloys [22] were also plotted for comparison. It is clear that κ can be significantly decreased with incorporation of Er atoms in InGaN alloys, particularly in those with low In content. High κ in undoped InGaN alloys of low In content is due to a weaker alloy scattering effect compared with that of InGaN alloys of higher In content. Incorporation of Er, a heavy element, provides additional scattering centers for phonons which further reduce κ . Such a reduction in κ due to Er doping has also been observed in InGaAs alloys [25]. The effect of Er for reducing κ in high In content was found to be less significant. This could be due to the alloy effect becoming more prominent as In content increases, which is expected to reach a maximum around middle of the In composition.

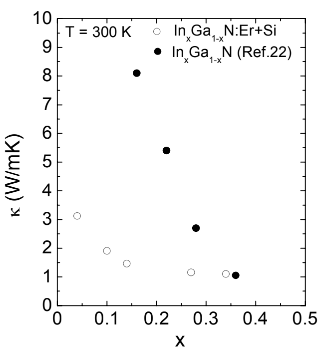

Fig. 2 Thermal conductivity (κ) of $In_xGa_{1-x}N$: Er + Si alloys vs. In content, x measured at room temperature. Solid dots are measured κ in undoped-In_xGa_1N alloys for comparison.

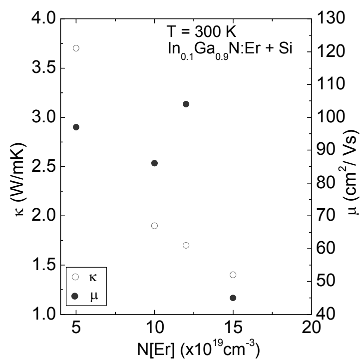

Fig. 3 Thermal conductivity (κ) of $In_xGa_{1-x}N$: Er + Si alloys as a function of Er concentration, N[Er] measured at room temperature.

Figure 3 shows κ and electron mobility μ of $In_{0.10}Ga_{0.90}N$: Er + Si as functions of Er concentration, N[Er]. μ was measured by Hall-effect measurement and N[Er] was measured by a secondary ion mass spectrometer (SIMS) measurement. N[Er] in $In_{0.10}Ga_{0.90}N$: Er + Si was found to be ~5 x 10^{19} cm^{-3} with an Er flow rate of 0.5 slm. We expect that N[Er] increases linearly as the Er flow rate increases in $In_{0.10}Ga_{0.90}N$: Er + Si alloys. It was observed that κ decreased significantly in $In_{0.10}Ga_{0.90}N$: Er + Si from 3.7 to 1.4 W/mK at room temperature while

μ decreased from 97 to 45 cm^2/ Vs as N[Er] increased from $5x10^{19}$ to $1.5x10^{20}$ cm^{-3}. Reduction in κ and μ with increasing N[Er] is due to increased scattering centers.

Figure 4 (a) shows Seebeck coefficient S and electrical conductivity σ of $In_{0.10}Ga_{0.90}N$: Er + Si alloys as functions of N[Er]. σ were measured by Van der Pauw Hall-effect experiment. As N[Er] increased S increased and σ decreased . Increase in S is due to a decrease of electron concentration while decrease in σ is due to a decrease of both μ and electron concentration as N[Er] is increasing. Power factor ($P = S^2 \sigma$) and ZT of $In_{0.10}Ga_{0.90}N$:Er + Si as functions of N[Er] are shown in Fig 4 (b). P decreased while ZT increased initially and then decreased as N[Er] increased. The reduction in P is due to a reduction in σ as N[Er] is increasing. The ZT was found to reach a maximum at N[Er] around $1x10^{20}$ cm^{-3} due to the combined effect of P and κ. A maximum value of ZT = 0.046 was obtained in the $In_{0.10}Ga_{0.90}N$: Er + Si at N[Er] around $1x10^{20}$ cm^{-3} at room temperature.

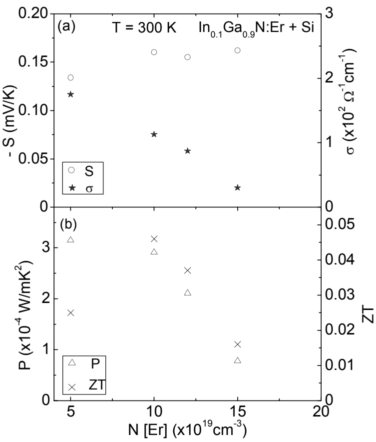

Fig. 4 (a) Seebeck coefficient, S and electrical conductivity, σ and (b) power factor, P and figure of merit, ZT of $In_xGa_{1-x}N$: Er + Si alloys as functions of Er concentration, N[Er] measured at room temperature.

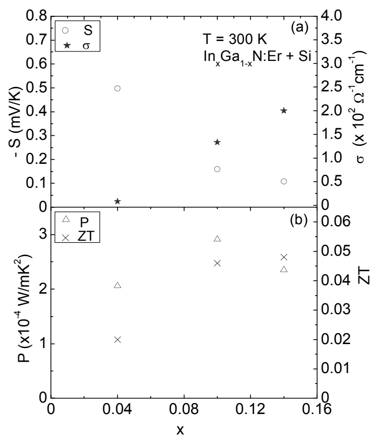

Fig. 5 (a) Seebeck coefficient, S and electrical conductivity, σ and (b) power factor, P and figure of merit, ZT of $In_xGa_{1-x}N$: Er +Si alloys as functions of In content, x measured at room temperature.

TE properties, S, σ, P, and ZT of $In_xGa_{1-x}N$: Er + Si ($0 \le x \le 0.14$) as functions of x are depicted in Fig 5 (a) and (b). The usual trade-off relationship between S and σ was observed. Increase in σ is due to an increase of eletron concentration with increasing x. ZT increases as In content increasing in $In_xGa_{1-x}N$:Er+Si ($0 \le x \le 0.14$) alloys. Beyond $x > 0.14$, we found significant reduction in μ, which results in lower ZT. Furthermore, the motivation of this work is to develop III nitride materials for high temperature TE applications. A ZT value of ~0.05 at room temperature was obtained in $In_{0.14}Ga_{0.86}N$: Er + Si which is much higher than that obtained in un-doped InGaN with similar In content [22]. Since low In content InGaN alloys can be stable at high temperatures, these Er doped InGaN alloys could be promising materials for high temperature applications.

CONCLUSIONS

In summary, TE properties of $In_xGa_{1-x}N$: Er + Si ($0 \leq x \leq 0.14$) alloys have been studied. It was found that doping of InGaN alloys with Er concentration, N[Er] larger than $5x10^{19}$ cm^{-3}, has substantially reduced the thermal conductivity κ in low In content InGaN alloys. Dependence of TE properties with N[Er] has been optimized in $In_{0.10}Ga_{0.90}N$: Er + Si alloys. The thermal conductivity κ decreased continuously as N[Er] increased in $In_{0.10}Ga_{0.90}N$: Er + Si alloys. The highest ZT was obtained at N[Er] about $1x10^{20}$ cm^{-3}. A room temperature ZT value of ~0.05 was obtained in $In_{0.14}Ga_{0.86}N$: Er + Si, which is much higher than that obtained in un-doped InGaN alloys with a similar In content. This indicates that InGaN: Er +Si alloys of low In content have potential for high temperature applications. Further improvement in ZT can be expected by improving material quality.

ACKNOWLEDGEMENTS

This research was supported by NSF (under Grant No. DRM-0906879). Jiang and Lin would like to acknowledge the support of the Whitacare Endowed Chair positions by the AT & T Foundation.

REFERENCES

1. T. M. Tritt, Science **283**, 804 (1999).
2. A. Boukai, K. Xu, and J. R. Heath, Adv. Mater. **18**, 864 (2006).
3. B. Poudel, Q. Hao, Y. Ma, Y. Lan, A. Minnich, B. Yu, X. Yan, D. Wang, A. Muto, D. Vashaee, X. Chen, J. Liu, M. Dressehaus, G. Chen, and Z. Ren, Science **320**, 634 (2008).
4. M. Ohtaki, K. Araki, and K. Yamamoto, J. Electron. Mater. **38**, 1234 (2009).
5. L. Shi, D. Li, C. Yu, W. Jang, D. Kim, Z. Yao, P. Kim, and A. Majumdar, J. Heat Transfer **125**, 881 (2003).
6. Q. He, Q. Hao, G. Chen, B. Poudel, X. Wang, D. Wang, and Z. Ren, Appl. Phys. Lett. **91**, 052505 (2007).
7. A. Charoenphakdee, K. Kurosaki, A. Harnwunggmoung, H. Muta, and S. Yamanaka, J. Alloys Compound **496**, 53 (2010).
8. D. M. Rowe and V. S. Shukla, J. Appl. Phys. **52**, 7421 (1981).
9. X. W. Wang, H. Lee, Y.C. Lan, G.H. Zhu, G. Joshi, D. Z. Wang, J. Yang, A. J. Muto, M. Y. Tang, J. Klatsky, S. Song, M. S. Dresselhaus, G. Chen, and Z. F. Ren, Appl. Phys. Lett. **93**, 193121 (2008).
10. I. M. Kokanbaev, J. Eng. Physics and Thermophysics **76**, 432 (2003).
11. J. W. Roh, S. Y. Jang, J. Kang, S. Lee, J. Noh, W. Kim, J. Park, and W. Lee, Appl. Phys. Lett. **96**, 103101 (2010).
12. A. Harnwunggmoung, K. Kurosaki, H. Muta, and S. Yamanaka, Appl. Phys. Lett. **96**, 202107 (2010).
13. M. Ohtaki, T. Tsubota, K. Eguchi, and H. Arai, J. Appl. Phys. **79**, 1816 (1996).

14. C. B. Satterthwaite and R. W. Ure, Phy. Rev. **108**, 1164 (1957).
15. R. Venkataubramanian, E. Siivoa, T. Colpitts, and B. O'Quinn, Nature **413**, 597 (2001).
16. L. M. Goncalves, C. Couto, P. Alpuim, A. G. Rolo, F. Volklein, and J. H. Correia, Thin Solid Flims **518**, 2816 (2010).
17. S. Yamguchi, R. Izaki, K. Yamagiwa, K. Taki, Y. Iwamura, and A. Yamamoto, Appl. Phys. Lett. **83**, 5398 (2003).
18. S. Yamagchi, Y. Iwamura, and A. Yamamoto, Appl. Phys. Lett. **82**, 2065 (2003).
19. A. J. Minnich, M. S. Dresselhaus, Z. F. Ren, and G. Chen, Energy Environ. Sci. **2**, 466 (2009).
20. J. Bahk, Z. Bian, M. Zebarjadi, J. M. O. Zide, H. Lu, D. Xu, J. Feser, G. Zeng, A. Majumdar, A. C. Gossard, A. Shakouri, and J. E. Bowers, Phys. Rev. B **81**, 235209 (2010).
21. A. Sztein, H. Ohta, J. Sonoda, A. Ramu, J. Bowers, S. DenBaars, and S. Nakamura, Appl. Phys. Express **2**, 111003 (2009).
22. B. N. Pantha, R. Dahal, J. Li, J. Y. Lin, H. X. Jiang, and G. Pomrenke, Appl. Phys. Lett. **92**, 042112 (2008).
23. B. N. Pantha, R. Dahal, J. Li, J. Y. Lin, H. X. Jiang, and G. Pomrenke, J. Electron. Mater. **38**, 1132 (2009).
24. G. D. Mahan, "Rare Earth Thermoelectrics," Proceedings of the 16th International Conference on Thermoelectrics, Dresden, Germany, 1997, pp. 21-24.
25. W. Kim, J. Zide, A. Gossard, D. Klenov, S. Stemmer, A. Shakouri, and A. Majumdar, Phys. Rev. Lett. **96**, 045901 (2006).
26. D. G. Cahill, Rev. Sci. Instrum. **61**, 802 (1990).
27. D. G. Cahill, M. Katiyar, and J. R. Ablson, Phys. Rev. B **50**, 6077 (1994).